J|A|C|S
COMMUNICATIONS

Published on Web 05/02/2007

Fatty Acid Salts as Stabilizers in Size- and Shape-Controlled Nanocrystal Synthesis: The Case of Inverse Spinel Iron Oxide

Maksym V. Kovalenko,* Maryna I. Bodnarchuk, Rainer T. Lechner, Günter Hesser, Friedrich Schäffler, and Wolfgang Heiss

Institute of Semiconductor and Solid State Physics, Johannes Kepler University Linz, A-4040 Linz, Austria

Received December 22, 2006; E-mail: maksym.kovalenko@jku.at

The development of efficient methods for the synthesis of nanostructures with well-defined sizes and shapes is one of the key trends in inorganic and physical chemistry. In the colloidal synthesis the choice of appropriate surfactants is crucially important for controlling the nucleation and growth as well as the crystal shape of the obtained nanocrystals (NCs).[1]

Oleic acid is one of the most widely employed surfactants for the synthesis of various NCs from metals,[2] II−VI, IV−VI, and III−V semiconductors,[3] and metal oxides.[4] The presence of a carboxylic group with significant affinity to various surfaces together with a nonpolar tail group for sterical hindering is the base for the excellent stabilizing function of this ligand. Commonly used approaches to further tailor the ligand performance of carboxylic acids are those based on the modifications of length or structure of the nonpolar group.[3e,5] Here we demonstrate, in contrast, that the variation of the cations of the oleate stabilizer can be an additional powerful tool to tailor the ligand performance, but without affecting the structure of the oleate. This approach enables the control of the reactivity (or activity) of the carboxylic group and as a result the nucleation and growth dynamics of the NCs. Such a control we show for iron oxide NCs, which are technologically very important because of various promising applications of them in high-density information storage[6] devices, for medical imaging and biotechnology.[7] By careful adjustment of the stabilizer composition as well as the reaction temperature profile we have obtained a size- and shape-controlled synthesis of monodisperse spherical, cubic, and bipyramidal iron oxide NCs.

For a synthesis of iron oxide (magnetite Fe_3O_4)[8,10] NCs we have adopted a method,[9] which is based on thermal decomposition of iron oleate precursors. In a typical experiment,[10] a solution containing iron oleate (0.2 mol/kg) and an equimolar amount of stabilizer in a high-boiling solvent was vacuum-dried at 120 °C and heated (3.3 °C/min) to reflux for 30 min to allow NC growth. Octadecence (bp = 318 °C) and its mixtures with diphenyl ether (bp = 259 °C) or tetracosane (bp = 391 °C) were used as solvents to adjust the reflux temperatures in the range of 290−375 °C and thus to control the size of the NCs. Sodium oleate (NaOL), potassium oleate (KOL), dibutylammonium oleate (DBAOL), and oleic acid (OA) were utilized as stabilizers. After cooling, iron oxide NCs were isolated applying a standard solvent/nonsolvent procedure,[3b] using hexane/ethanol (smaller NCs) or chloroform/acetone (larger NCs) pairs.

Cubic NCs of 9−23 nm were obtained in the presence of NaOL as stabilizer (Figure 1). They exhibit narrow size distributions (size deviation $\sigma = 5-8\%$[10]), aspect ratios close to one (Figure 1f and Figure S1 in Supporting Information), sharp edges, and flat facets with only atomic steps (Figures 1g and S4). The HRTEM analysis (Figures 1g, 1h, and S4) shows that these NCs are single-crystalline, {100}-bound cubes with an interplanar spacing of 2.92 and 4.9 Å for the {220} and {111} planes, respectively, which is consistent

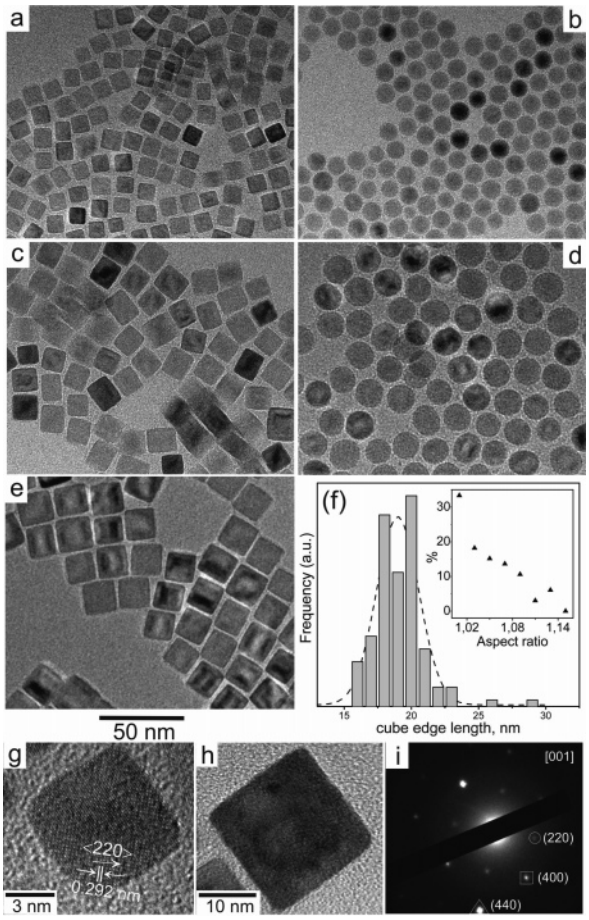

Figure 1. TEM images of monodisperse cubic (a, c, e) and spherical (b, d) iron oxide NCs, size-histogram of cubic NCs (f), HRTEM images of 7.7 nm (g) and 21.8 nm (h) cubic NCs, and electron diffraction pattern (with [100] zone axis) from a single iron oxide nanocube (i).

with the bulk values of iron oxide with inverse spinel structure. KOL shows a similar effect on the iron oxide NC shape and mixtures of cubes with other faceted but somewhat irregularly-shaped particles are typically obtained (Figure S6). In contrast, both OA and DBAOL induce growth of monodisperse ($\sigma = 4-6\%$) spherical particles in the same range of sizes (Figures 1b,d, S2).

Further adjustments of the synthetic conditions[10] give rise to a high yield (~50%) of NCs, which appear as various triangular projections in the TEM images (Figure 2a) mixed with cubic NCs. A detailed HRTEM analysis (Figures 2b, c) together with TEM imaging under various tilt angles (Figure S7) and dark-field imaging (Figure S8) provides that these NCs are {100}-bound bipyramides with a single (111) twin plane, bisecting them into two halves. Remarkably, this shape is identical to those recently reported for silver NCs.[11] The contact (111) twins are well-known for bulk

10.1021/ja0692478 CCC: $37.00

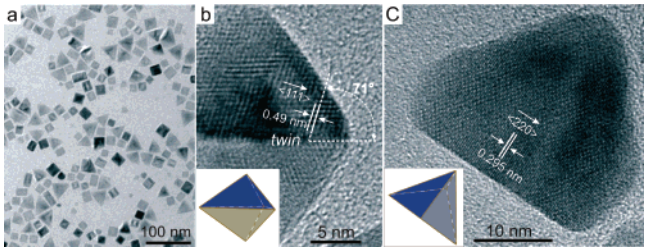

Figure 2. TEM (a) and HRTEM (b, c) images of bipyramidal iron oxide NCs. An angle of 71° is close to the theoretical angle of 70.5° between (111) planes.

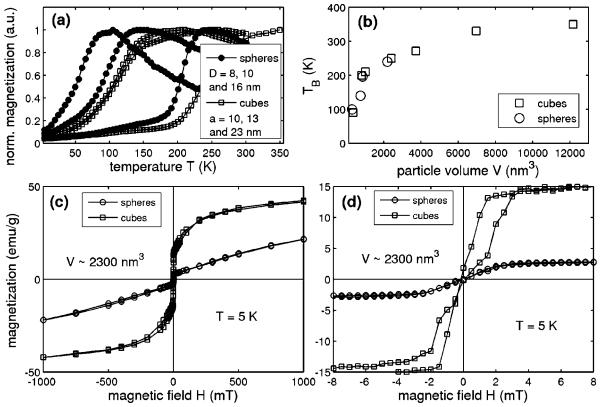

Figure 3. (a) DC-magnetization vs temperature T for spherical NCs (●) with diameters $D = 8$, 10, and 16 nm and for nanocubes (□) with edge lengths $a = 10$, 13, and 23 nm measured at a magnetic field H of 10 mT. (b) Blocking temperature T_B derived from the maxima in panel a as a function of NC volume V. (c) Magnetization vs H-field for cubes (□) and spheres (○) with nearly the same volumes measured at $T = 5$ K. (d) Zoom of panel c.

magnetite but, as far as we know, they were not reported for iron oxide NCs. The probability of obtaining single twinned seeds for the growth of bipyramidial NCs depends simultaneously on several factors like heating rate and NaOL concentration.[10]

The magnetic properties of the shape-controlled NCs are summarized in Figure 3. Above the blocking temperatures T_B, all samples show superparamagnetic magnetization curves, shown exemplarily in Figure S9. The T_B values of the NCs, derived from the maxima of the DC-magnetization curves (Figure 3a) increase with increasing particle volume from 90 to 350 K, independently from the particle shape (Figure 3b). For the 35 nm large bipyramides T_B exceeds 350 K (Figure S10). In contrast, the magnetic behavior below T_B shows pronounced shape dependence. The 5 K magnetization as function of the magnetic field saturates above 200 mT for 13 nm cubes (Figure 3c). For the 16 nm spheres with almost the same volume, however, saturation is achieved well above 1 T. For small fields also, different magnetization behaviors are observed (Figure 3d). The cubes depict pronounced hysteresis loops around ±1.5 mT and exhibit no remanence or coercivity, not shown by the spheres.

The cubical shape of the NCs is a result of a slower growth rate for the {100} facets as compared to all other facets.[12] In the present synthesis, the anisotropy of the growth rate can be attributed to a different adhesion of the stabilizer on the growing surface, since the stabilizer species is the only parameter which was changed to obtain cubical shapes instead of spheres. Replacing OA by its salts allows us to vary the concentration of "free" oleate ions or those bound in loose ionic pairs over a wide range, as is evidenced by conductivity measurements at elevated temperatures. The conductivity measurements (Figure S11) show above 220−230 °C significant electrolytic dissociation for the oleates resulting in cubic NCs (NaOL and KOL), whereas both OA and DBAOL giving spherical shapes remain in molecular form. A strong concentration dependence of the facet-selective ligand adsorption is commonly observed,[1b,13] and for spinel-structured $MnFe_2O_4$,[14] which is very similar to magnetite, a transition to cubic shape is also observed with increasing oleate concentration.

In conclusion, various oleic acid salts act as stabilizers for the size- and shape-controlled synthesis of iron oxide NCs. Novel shapes for superparamagnetic iron oxide NCs, such as cubes and bipyramids with different magnetization properties at low temperatures, are demonstrated, enlarging the family of well-defined NC shapes for inverse spinel iron oxides.[4f,15] These results suggest the general applicability of oleic acid salts as stabilizers in well-controlled NC syntheses.

Acknowledgment. Financial support from the Austrian Science Foundation FWF (START Y179 and SFB-IRON) and the Austrian Nano Initiative (NSI:Nanoshape) is acknowledged.

Supporting Information Available: Experimental details, more TEM, HRTEM and electron diffraction data, magnetization curves, and further discussions. This material is available free of charge via the Internet at http://pubs.acs.org.

References

(1) (a) Yin, Y.; Alivisatos, A. P. *Nature* **2005**, *437*, 664−670. (b) Jun, Y.-W.; Choi, J.-S.; Cheon, J. *Angew. Chem., Int. Ed.* **2006**, *45*, 3414−3439.

(2) (a) Sun, S.; Murray, C. B.; Weller, D.; Folks, L.; Moser, A. *Science* **2000**, *290*, 1989−1992. (b) Wu, Y.; Li, Y.; Ong, B. S. *J. Am. Chem. Soc.* **2006**, *128*, 4202−4203. (c) Puntes, V. F.; Krishnan, K. M.; Alivisatos, A. P. *Science* **2001**, *291*, 2115−2117.

(3) (a) Hines, M. A.; Scholes, G. D. *Adv. Mater.* **2003**, *15*, 1844−1849. (b) Murray, C. B.; Sun, S.; Gaschler, W.; Doyle, H.; Betley, T. A.; Kagan, C. R. *IBM J. Res. Dev.* **2001**, *45*, 47−55. (c) Yu, W. W.; Peng, X. *Angew. Chem., Int. Ed.* **2002**, *41*, 2368−2371. (d) Bullen, C. R.; Mulvaney, P. *Nano Lett.* **2004**, *4*, 2303−2307. (e) Battaglia, D.; Peng, X. *Nano Lett.* **2002**, *2*, 1027−1030.

(4) (a) Cozzoli, P. D.; Kornowski, A.; Weller, H. *J. Am. Chem. Soc.* **2003**, *125*, 14539−14548. (b) O'Brien, S.; Brus, L.; Murray, C. B. *J. Am. Chem. Soc.* **2001**, *123*, 12085−12086. (c) Hyeon, T.; Chung, Y.; Park, J.; Lee, S. S.; Kim, Y.-W.; Park, B. H. *J. Phys. Chem. B* **2002**, *106*, 6831−6833. (d) Sun, S.; Zeng, H.; Robinson, D. B.; Raoux, S.; Rice, P. M.; Wang, S. X.; Li, G. *J. Am. Chem. Soc.* **2004**, *126*, 273−279. (e) Hyeon, T.; Lee, S. S.; Park, J.; Chung, Y.; Na, H. B. *J. Am. Chem. Soc.* **2001**, *123*, 12798−12801. (f) Cozzoli, P. D.; Snoeck, E.; Garcia, M. A.; Giannini, C.; Guagliardi, A.; Cervellino, A.; Gozzo, F.; Hernando, A.; Achterhold, K.; Ciobanu, N.; Parak, F. G.; Cingolani, R.; Manna, L. *Nano Lett.* **2006**, *6*, 1966−1972.

(5) Shevchenko, E. V.; Talapin, D. V.; Schnablegger, H.; Kornowski, A.; Festin, O.; Svedlindh, P.; Haase, M.; Weller, H. *J. Am. Chem. Soc.* **2003**, *125*, 9090−9101.

(6) Cornell, R. M.; Schwertmann, U. *The Iron Oxides: Structure, Properties, Reactions, Occurrence and Uses*; VCH: Weinheim, Germany, 1996.

(7) Hafeli, U.; Schutt, W.; Teller, Zborowski, M. *Scientific and Clinical Applications of Magnetic Carriers*; Plenum Press: New York, 1997.

(8) Owing to the presence of $Fe^{2+}-Fe^{3+}$ charge-transfer transitions observed by infrared absorption measurements, our NCs are close to magnetite, which is in agreement with ref 9a, where also a synthesis based on the decomposition of presynthesized iron oleate is used.

(9) (a) Park, J.; An, K.; Hwang, Y.; Park, J.-G.; Noh, H.-J.; Kim, J.-Y.; Park, J.-H.; Hwang, N.-M.; Hyeon, T. *Nat. Mater.* **2004**, *3*, 891−895. (b) Jana, N. R.; Chen, Y.; Peng, X. *Chem. Mater.* **2004**, *16*, 3931−3935. (c) Yu, W. W.; Falkner, J. C.; Yavuz, C. T.; Colvin, V. L. *Chem. Commun.* **2004**, *14*, 2306−2307.

(10) For more details see Supporting Information.

(11) Wiley, B. J.; Xiong, Y.; Li, Z.-H.; Yin, Y.; Xia, Y. *Nano Lett.* **2006**, *6*, 765−768.

(12) Wang, Z. L. *J. Am. Chem. Soc.* **2000**, *104*, 1153−1175.

(13) Yu, D.; Yam, V. W.-W. *J. Am. Chem. Soc.* **2004**, *126*, 13200−13201.

(14) Zeng, H.; Rice, P. M.; Wang, S. X; Sun, S. *J. Am. Chem. Soc.* **2004**, *126*, 11458−11459.

(15) (a) Zheng, R.; Gu, H.; Xu, B.; Fung, K. K.; Zhang, X.; Ringer, S. P. *Adv. Mater.* **2006**, *18*, 2418−2421. (b) Cheon, J.; Kang, N.-J.; Lee, S.-M.; Lee, J.-H.; Yoon, J.-H.; Oh, S. J. *J. Am. Chem. Soc.* **2004**, *126*, 1950−1951.

JA0692478